ORIGINAL PAPER

Long-term Effects of Recurrent Neonatal Seizures on Neurobehavioral Function and Related Gene Expression and Its Intervention by Inhibitor of Cathepsin B

Hong Ni · Jian-zhen Yan · Le-ling Zhang ·
Xing Feng · Xi-ru Wu

Abstract Cathepsins are families of proteases that have been reported to play the key roles in neuroexcitotoxicity. The present study was sought to determine the effect of CBI, a cathepsin B inhibitor, in the prevention of neurobehavioral deficits after inhalant flurothyl-induced recurrent neonatal seizures in rats. We examined the expression pattern of autophagy-related genes at acute phase after the last seizures using western blot method, and evaluated behavioral deficits during postnatal day 28 (P28) to P35. The results showed improved neurological scores and learning ability in CBI-treated rats compared with the nontreated control. Flurothyl-induced increases in the ratio of LC3-II/LC3-I, Beclin-1 and Cathepsin-B were blocked by pre-treatment with CBI at 1.5, 3, 6 and 24 h after the last seizures in hippocampus and cerebral cortex by western blot analysis. Meanwhile, CBI also reversed flurothyl-induced down-regulation of Bcl-2 protein levels. Furthermore, in the long-term time point of 35 days (P35), PRG-1 mRNA and protein level in hippocampus and cerebral cortex of recurrent seizure group were up-regulated when compared to the control rats; meanwhile, the up-regulated expression of PRG-1 were robustly inhibited by CBI. These date demonstrated, for the first time, that lysosomal enzymes participate in neonatal seizure-induced brain damage and that modulation of cathepsin B may offer a new strategy for the development of therapeutic interventions for treatment of developmental seizure-induced brain damage.

Introduction

Developmental seizure-induced excitotoxicity plays a general role in pathophysiologic responses that led to subsequent cognitive deficit as observed in human patients and rat models [1–3]. Morphological and biochemical approaches have shown the presence of both apoptotic and autophygic neuron death in striatum and hippocampus after kainic acid or flurothyl-induced seizure injury [4, 5] As few anti-apoptotic therapies have proven to be useful in inhibiting seizure injury, therefore, autophagy-mediated apoptosis has been intensively studied in recent years and may be a potential target for developing a novel therapy for seizure damage.

Autophagy is a homeostatic and dynamic process for intracellular recycling of bulk proteins and aging organelles. Increased autophagy has been reported in experimental models of excitotoxicity such as stroke, and in patients with Alzheimer's disease and critical illness [6]. For example, we have previously demonstrated in rat models that autophagic pathway is activated immediately after seizure, ischemia, neurodegenerative and traumatic brain injury [4, 5, 7, 8]. Besides, a lysosomal-apoptosis axis theory of cell death has also been proposed [9]. Apoptotic neuron deaths after pathologic brain injury is accompanied

H. Ni (✉) · J. Yan · L. Zhang · X. Feng
Neurology Laboratory, Soochow University Affiliated
Children's Hospital, No. 303, Jingde Road, 215003 Suzhou,
People's Republic of China
e-mail: nyr2000@yeah.net; nhdoctor@163.com

H. Ni · J. Yan · L. Zhang · X. Feng
Institute of Neuroscience, Soochow University, 215003 Suzhou,
People's Republic of China

X. Wu
Department of Pediatrics, First Hospital Affiliated to Peking
University, 100034 Beijing, China

by the activation of autophygic/lysosomal system, which may be associated with proapoptotic factors such as auto-phygic marker LC3, beclin-1, Cathepsin-B and suppressed by anti-apoptotic factors such as Bcl-2. For instance, our recent study in kainic acid or traumatic brain injury (TBI) model has demonstrated that lysosomal protease Cathep-sin-B is co-activated with autophygic and apoptotic path-ways [4, 8]. We thus predict that the interaction of lysosomal with autophagic and apoptotic signals may exist in experimental developmental seizure model. To test this hypothesis, we asked whether/how seizure injury may affect key components of autophagic pathways, such as lysosomal family (cathepsin B), the major executioners of autophagic pathway (LC3, beclin-1),and anti-apoptotic marker bcl-2, along with plasticity related gene 1 (PRG-1) in rat brains.

CBI is a specific inhibitor of Cathepsin B, a lysosomal cysteine protease, can protect cells against excitotoxic hippocampal or striatal neuronal death [4, 8]. But the contribution of CBI to developmental seizure-induced brain damage and the underlying molecular mechanism, however, has never been studied. Here, we used CBI to investigate the role of cathepsin-B in seizure-induced cognitive deficit, as well as expression of proteins involved in autophagy, apoptosis, and lysosome functions.

Intriguingly, we found that CBI treatment could protect seizure-induced neuronal dysfunction, potentially through regulation of key components in lysosomal pathways. These results raised the possibility that Cathepsin B inhibitors can be developed as pharmaceutical treatments for seizure-induced brain injury.

Methods and Materials

Animal Preparation

Sprague–Dawley rats were used in all experiments and were treated in accordance with the guidelines set by the National Institutes of Health for the humane treatment of animals. Attempts were made to minimize the number of animals used. Ninety Sprague–Dawley neonatal rats at postnatal day 6(P6) were randomly divided into three groups: the recurrent-seizures group (RS, n = 30), the CBI treated-seizure group (CBI group, each rat was pretreated with CBI before seizures were induced, total volume 2/μl, concentration 0.5 μg/μl, Santa Cruz Biotechnology, Santa Cruz, CA; i.p., n = 30) and the control group (n = 30).

The procedure of seizure induction has been described in detail previously [10, 11]. Briefly, seizures were induced in the neonatal rats with volatile flurothyl (bis-2, 2, 2-tri-flurothyl ether, Aldrich-Sigma Chemical, WI, USA), a potent and rapidly acting central nervous system stimulant

that produces seizures within minutes of exposure. The pups were put into a transparent plastic airtight box and liquid flurothyl was delivered through a syringe and drip-ped at a rate of three drops/min onto filter paper in the center of the container where the agent evaporates. Experimental rats were exposed to flurothyl until tonic extension of both the forelimbs and hindlimbs was observed. The rats were then quickly removed from the chamber and allowed to recover in room air until the ani-mals returned to their baseline activity level. Control rats were placed into the container for an equal amount of time without exposure to flurothyl and were separated from their dam for the same duration as rats exposed flurothyl. The experimental rats had 45 induced seizures during the nine consecutive days, from P6 to P14. Rats had 5 seizures/day for nine consecutive days, with a minimum of 30 min between seizures. The rats had access to food and water ad libitum and were housed with their littermates until weaning at P21. They were group-housed in plastic cages on a standard 12/12 h light/dark cycle.

Western Blot Analysis

At 1.5, 3, 6 and 24 h after the last seizure, rats (n = 72) from flurothyl-treated RS group (n = 24), CBI group (n = 24) and control (n = 24) were sacrificed. The hip-pocampus and cerebral cortex in every time point from each group (number = 6) were rapidly removed and immediately frozen in dry ice for western blot analysis as described by Luo [8]. Tissue samples were homogenized in Western blot lysis buffer containing 10 mM Tris–HCl (pH 7.4), 150 mM NaCl, 1% Triton X-100, 1% sodium deoxycholate, 0.1% SDS, 5 mM EDTA, 1 mM PMSF, 0.28 ku/l aprotinin, 50 mg/l leupeptin, 1 mM benzamidine, and 7 mg/l pepstain A. The homogenate was then centrifuged at $10,600 \times g$ for 10 min at 4°C and supernatant was preserved at −70°C for last use. Protein concentration was determined using a BCA kit (Pierce). Thirty micrograms of protein from each sample was subject to electrophoresis on 10% SDS-PAGE gel using a constant current. Proteins were electrotransferred onto polyvinylidene fluoride membranes. After blocking with a blocking solution TBS-T containing 20 mM Tris base, 137 mM sodium chloride, 5% non-fat milk powder and 0.05% Tween 20 overnight at 4°C, blots were then incubated with one of the following antibodies: a goat polyclonal antibody against MAPLC3B (Santa Cruz Biotechnologies, Santa Cruz, CA), a goat polyclonal antibody against beclin 1 (Santa Cruz Biotech-nologies), a goat polyclonal antibody against cathepsin B (Santa Cruz Biotechnologies), a rabbit polyclonal antibody against Bcl-2 (Santa Cruz Biotechnologies), rabbit anti-PRG-1 polyclonal antibody (1:1000, GenScript) in Tris buffered saline containing 0.2% Tween-20 (TBST) and 3%

nonfat dry milk for 3 h. The blot was washed several times with TBS-T and then incubated with horseradish peroxidase-conjugated secondary antibody in TBST for 2 h (1:10,000, Santa Cruz). Specific bands were visualized on a film Kodak X-Omat LS using the ECL detection system Amersham. The relative changes of the intensity of each immunoreactive band were evaluated with Sigma Scan Pro 5 and were normalized to a loading control β-actin.

Morris Water Maze Test

During adolescence (P28-P34), a subset of rats (n = 6 each group) underwent testing in the Morris water maze to assess visual-spatial learning and memory. The procedure has been described in detail [12, 13]. Briefly, for the place navigation (spatial learning acquisition) test, each animal was subjected to two trials per day. Each trial consisted of placing the rat in water facing the wall of the pool at one of the four starting locations (North, East, South and West) in a random order. The rat was allowed to search the platform for a maximum of 60 s. If an animal did not find the platform in 60 s, it was gently lifted up and placed onto the platform for 60 s before being returned to the cage. The swim paths were automatically recorded by a video/computer system. The swim paths are defined as 4 swim strategies by the software: (1) marginal, swimming along the pool edge; (2) random, swimming randomly; (3) taxis, swimming around but generally towards the platform area; (4) straight, swimming straight toward the platform. The first two strategies are inefficient and the last one is the most efficient in searching for the platform. We recorded the frequency (number of times) of passing through the platform quadrant, and analyzed the frequency to reflect the spatial memory ability. The times of each strategy used by each rat in 2 trials per day were recorded and then calculated.

Spatial Probe Test: Remove the hidden platform on alternate days after the navigation test (P34), and then place the rat into the water from the middle point of the edge in the target quadrant and allowing the rat to swim for 60 s in search of it. We recorded the frequency (number of times) of passing through the platform quadrant, and analyzed the frequency to reflect the spatial memory ability.

Open Field Test

At P35 rats were evaluated for activity level in the open field test. The procedure has been described in detail [11]. The rats were placed in a closed area with the floor divided into 64 equal squares (100 cm^2). The number of squares crossed in 2 min was measured on the day of testing. The testing area was cleaned after each trial and ambient lighting and noise remained constant throughout both testing days. Testing was done between 0,900 and 1,000.

Real-time RT-PCR or Western Blot Study

After the behavioral tests, rats were anesthetized with chloropent (3 ml/kg, i.p.). The hippocampus and cerebral cortex tissue samples dissected from fresh brain were rapidly removed and immediately frozen in dry ice. Total hippocampal and cerebral cortex samples from the right hemisphere (the samples from left hemisphere was used for western blot analysis) was extracted from each sample using TRIZOL reagent (InVitrogen Life Technologies. USA) according to the manufacture's instruction and dissolved in DEPC-treated water. The concentration, purity and amount of total isolated RNA were determined by ultraviolet spectrophotometry. By these standards, all the RNA samples used for assay were of high quality and purity by measuring OD at 260 nm and 280 nm (Abs260/Abs280 > 1.8). Two micrograms of total RNA was reverse transcribed into cDNA by using random primers, 200U of MMLV reverse transcriptase (InVitrogen, USA), 0.5 mM dNTPs, 10 mM dithiothreitol, and 25 U of Rnase inhibitor (InVitrogen). Forty microliter RT reaction was performed at 37°C for 60 min, then at 95°C for 5 min. RT products were stored in −20°C until assayed.

RT-PCR was carried out using TaqMan probe-based chemistry (Applied Biosystems, Foster City, CA, USA). The primers and probes of the twenty genes were designed against GenBank-published sequences with the software Primer Express 2.0 (Applied Biosystems), of which the sequences were listed in Table 1. The amplification reactions (25μl) contained 1 × buffer, final concentrations of 4 mM MgCl$_2$, 0.2 mM dNTPs, 0.3 μM primers, 1U Taq DNA polymerase, 200 nM TaqMan probe, and 50 ng cDNA template. Reactions were performed on an ABI Prism 5700 Sequence Detector (Applied Biosystems) in a universal two-step procedure. The closed tubes were incubated at 94°C for 5 min, and then followed by denaturing at 94°C, annealing and elongation at 60°C for 45 cycles. Real-time fluorescent data were collected and analyzed with SDS1.3 software. The ΔCT method of relative quantification was used to determine the fold change in expression. This was done by first determining the real-time PCR threshold cycle (CT) of the target mRNAs and the internal control β-actin. Then the ratio target genes: β-actin were calculated as follows: target genes: β-actin = $2^{CT \ (target)-CT \ (\beta\text{-actin})}$ (ΔCT = CT Target−CT β-actin). The fold change in expression was then obtained ($2^{-\Delta CT}$ –method) [12].

Statistical Analysis

The escape latency of place navigation test, the frequency of passing through the platform quadrant of spatial probe test in the water maze and the number of squares crossed in

Table 1 Oligonucleotide primers for real-time RT-PCR analysis

Gene	Genbank accession number	Primer sequence	No.of cycles
LC-3	NM_012823	F: 5′-CCTGCTGCTGGCCGTAGT-3′	45
		R: 5′-TGATGAAGTCTTCCTGCCAAAA-3′	
		Probe: 5′-FAM-CGCTGTACGAGGAACACCCCAGCT-TAMRA-3′	
Cathepsin-B	NM_022597	F: 5′-GGGAACAGTGGTCCAATTGC-3′	45
		R: 5′-CCCCAAATGCCCAACAAG-3′	
		Probe: 5′-FAM-CGACCATCGCACAGATCAGAGACCAG-TAMRA-3′	
PRG-1	AF541280	F: 5′-TTGTTCGGGATCTGACCTAACA-3′	45
		R: 5′-AGCGAGGGTCGCATGCT-3′	
		Probe: 5′-FAM-AACAATGGCAAAAAGTCATTCCCGT-TAMRAM-3′	

open field test were analyzed with post hoc comparisons using a Bonferroni test after ANOVA. The protein levels, gene expression levels ($2^{-\Delta CT}$) and the searching strategies in the water maze were compared by nonparametric Kruskal–Wallis test using SAS 8.0 statistical software. Data was presented as the mean with SD and statistical significance was considered as a *P < 0.05*.

Results

Features of the Rats with Flurothyl-Induced Seizures

The seizures were stereotyped as described by de Roqalski Landrot [10]. The rat pups showed signs of the seizure attacks which were characterized by clonic movements of the four limbs and loss of posture. Mild perioral cyanosis, urinary and fecal incontinence, and salivation were often noted. Rats were removed from the chamber as soon as the tonic phase began and allowed to recover in room air. Typically the rats returned to baseline behavior within 10–15 min. All pups survived as did the normal controls.

Physical and Mobility Landmarks

There were no significant differences among the three groups with regard to the physical and mobility landmarks, such as pinna unfolding, hair emergence, incisor eruption, eye opening and air righting reflex (data not shown).

Western Blot Analysis

Significant increases in the ratio of LC3-II/LC3-I (Fig. 1), beclin-1, Cathepsin-B and decreases in bcl-2 in hippocampus (Fig. 1) and cerebral cortex (Fig. 2) were observed at 1.5, 3, 6 and 24 h after the last seizures. Up-regulation of LC3, beclin-1, Cathepsin-B and down-regulation of bcl-2 were blocked by pretreatment with CBI. In addition, there

was a remarkable increase in the protein level of PRG-1 at P35 in hippocampus and cerebral cortex in RS group compared with that in the control and the CBI-treated groups (Fig. 3).

Morris Water Maze

There was a decreasing incidence of marginal strategy and an increasing trend in the use of taxis and straight line strategy in all three groups. However, the frequency of marginal strategy was higher and the frequency of taxis strategy was lower in RS group than that in CBI and control group in the second, third and fifth day ($P < 0.05$) (Fig. 4a–e). In addition, although rats in all three groups demonstrated learning in the water maze with decreasing latencies to platform with increasing days of training in the Morris maze test, however, the latencies of the RS group were significantly longer than those of control and 3-CBI groups in d5 ($P < 0.05$)of the test (Fig. 4f).

As far as Spatial Probe Test was concerned, the frequency of passing through the platform quadrant had no significant difference among three groups ($P > 0.05$).

Open Field Test

The blocks vertical crossed in RS group (2.5 ± 2.4) were significantly decreased compared with that in control (22.2 ± 10.7) and CBI groups (9.3 ± 5.4).

Real-time RT-PCR Analysis

The mRNA level of PRG-1 in hippocampus and cerebral cortex at P35 was significantly higher than that in control and CBI groups ($P < 0.05$) (Fig. 5).There were no significant difference in LC-3 and Cathepsin-B levels in both hippocampus and cerebral cortex among three groups (Fig. 5).
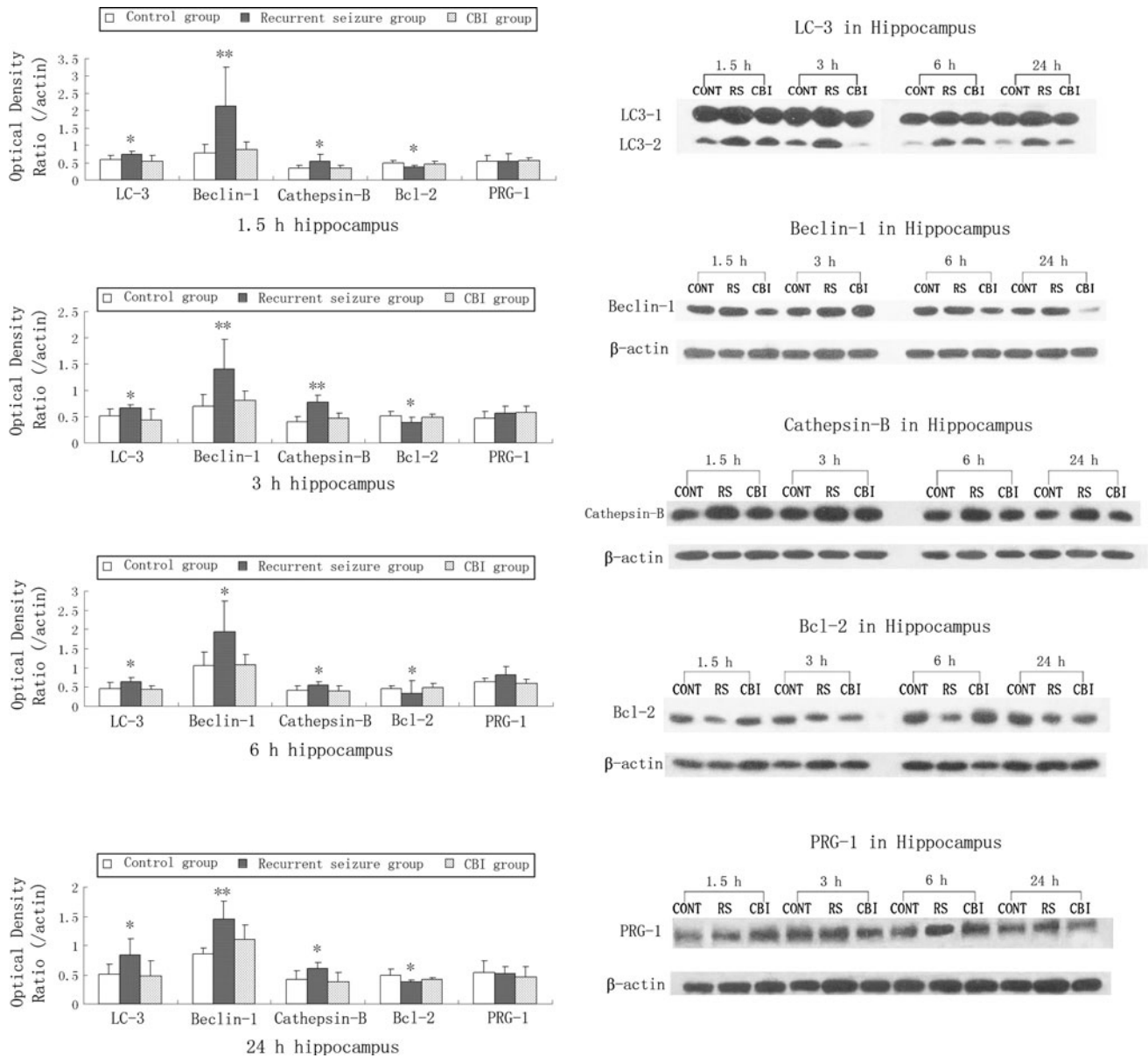
Fig. 1 Reversal of recurrent neonatal seizure-induced increase in LC3, beclin-1, cathepsin-B and decline in bcl-2 protein levels by CBI at 1.5, 3, 6 and 24 h after the last seizures. Extracts from the RS, CBI and control hippocampus were separated on SDS-PAGE, and protein levels were detected with western blot analysis. Statistical comparisons were carried out by nonparametric Kruskal–Wallis test. $**P < 0.01$ versus control and CBI groups; $*P < 0.05$ versus control and CBI groups

Discussion

We have previously characterized the neurobehavioral and histopathological effects of flurothyl seizure-induced brain damage, with an emphasis on a phenotypic anchor of excitatory/inhibitory gene expression to neurobehavioral injury, especially cognitive deficit [11, 14, 15]. However, the impact of neonatal seizures on autophagic gene expression has not been characterized and the question remains as to whether or not autophagic mechanism participates in developmental seizure-induced brain damage.

To support their contention, we used a cathepsin B inhibitor (CBI) to pretreat rats on postnatal day 6 intraperitoneally and then treat with flurothyl in the present study. The expression pattern of autophagic proteins, lysosome marker and anti-apoptotic marker are tested in hippocampus and cerebral cortex at 1.5, 3, 6 and 24 h after the last seizures. Analysis of Western blot showed that Beclin-1 and LC3 as well as Cathepsin-B are reduced significantly, but Bcl-2 protein and and plasticity related gene 1 (PRG-1) is elevated in in CBI-treated rats compared with the non-treated seizure group. In addition, neurological scores and
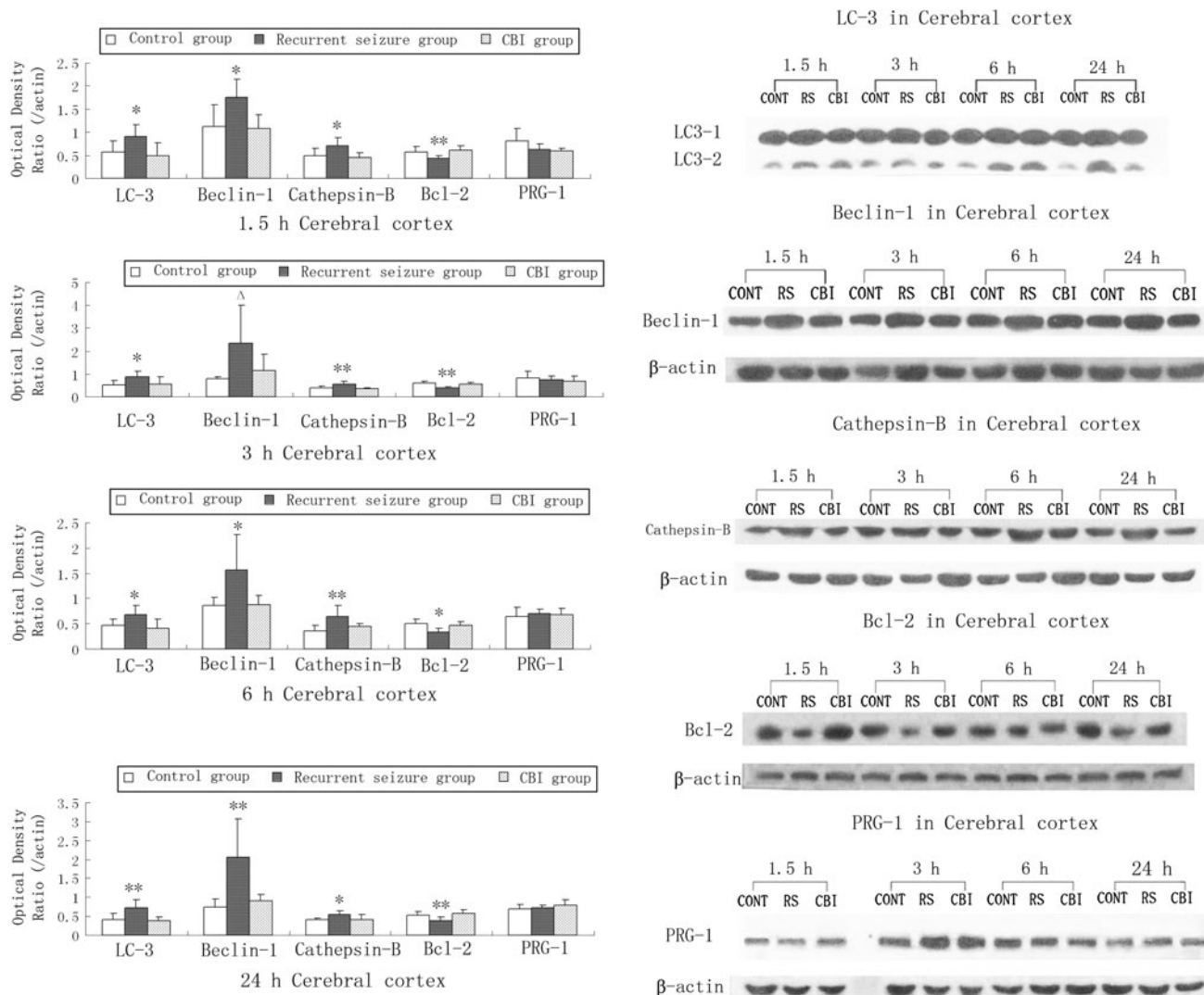
Fig. 2 Reversal of recurrent neonatal seizure-induced increase in LC3, beclin-1, cathepsin-B and decline in bcl-2 protein levels by CBI at 1.5, 3, 6 and 24 h after the last seizures. Extracts from the RS, CBI and control cerebral cortex were separated on SDS-PAGE, and protein levels were detected with western blot analysis. Statistical comparisons were carried out by nonparametric Kruskal–Wallis test. **$P < 0.01$ versus control and CBI groups; *$P < 0.05$ versus control and CBI groups; $^{\Delta}P < 0.05$ versus control

learning ability in CBI-treated rats are improved compared with the nontreated seizure group by Morris water maze task and open field test.

As reported, a substantial number of degenerating neurons within limbic regions display morphological features of apoptosis following prolonged seizures evoked by systemic or local injections of kainic acid, systemic injections of pilocarpine and sustained stimulation of the perforant path [16, 17]. It has also been found that autophagy was increased in rats with pilocarpine or KA-induced status epilepticus [18]. LC3 is the most reliable cellular marker for autophagy activation at present. LC3-II is the cleaved and lipidated form of the cytosolic LC3-I. LC3-II is the required for the formation of autophagosomes and has been defined as a marker of autophagosomes in mammalian cells

[19]. Beclin-1, another marker of autophagy is a component of the phosphatidylinositol-3- kinase complex that is required for autophagy [20]. Enhanced beclin-1 expression has been recently used as a marker of autophagy after closed brain injury [21], myocardial ischemia [22] and focal cerebral ischemia [23, 24]. So it is not surprising as autophagy/lysosomic marker (LC3, Beclin-1 and cathepsin-B) protein increased immediately following neonatal seizures in the present study. This is consistent with our previously reported findings in acute toxicity studies with flurothyl-induced recurrent neonatal seizures which revealed up-regulated expressions of ZnT-1, ZnT-2, LC3 and beclin-1 of RS group. Pre-treatment with 3-MA remarkably attenuated seizure-induced ZnT-1, ZnT-2, LC3 and beclin-1 increase [5]. Additionally, linear correlations
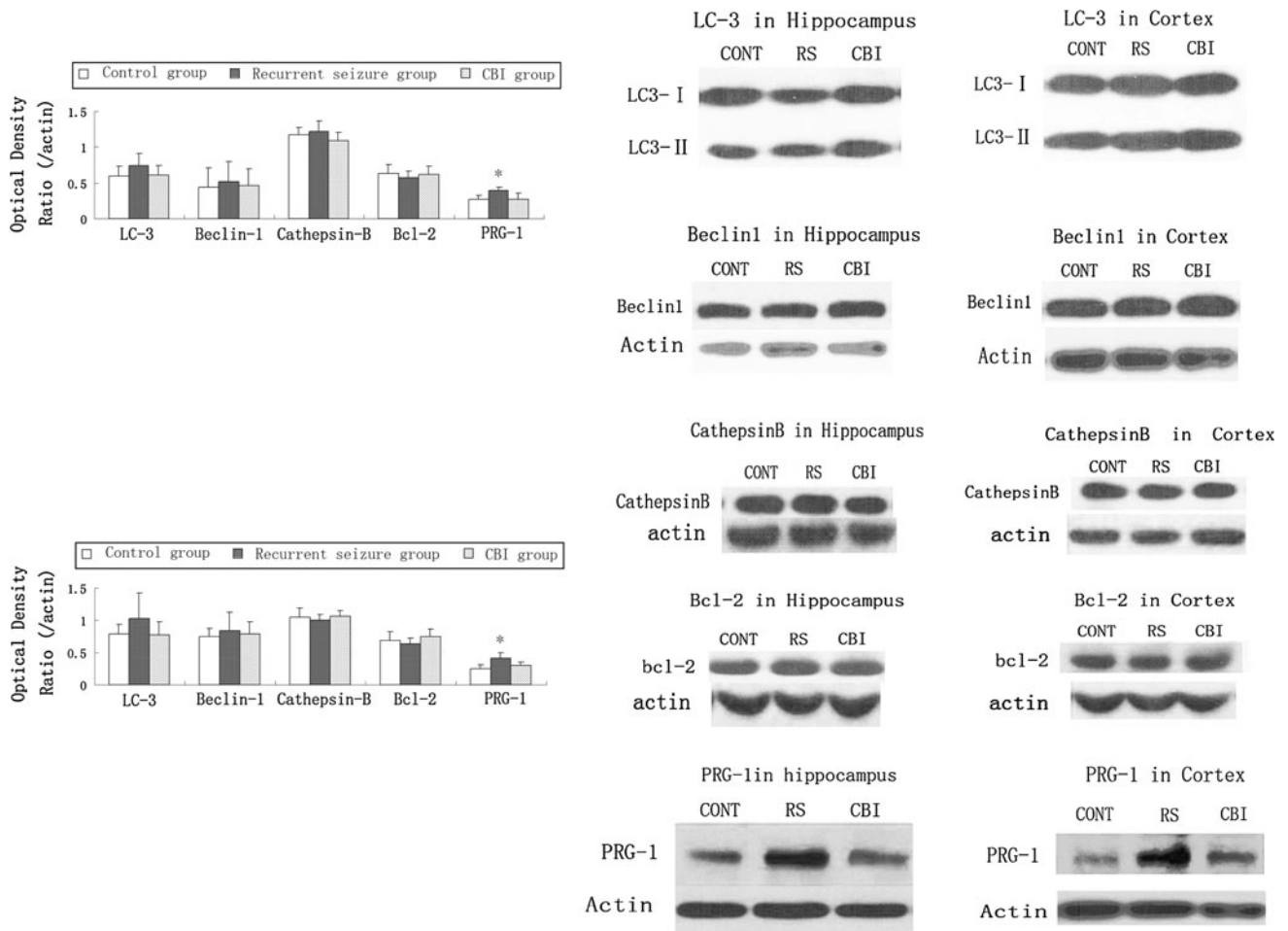
Fig. 3 Reversal of recurrent neonatal seizure-induced increase in PRG-1 protein levels by CBI at P35. Extracts from the RS, CBI and control hippocampus and cerebral cortex were separated on SDS-PAGE, and protein levels were detected with western blot analysis. Statistical comparisons were carried out by nonparametric Kruskal–Wallis test. *$P < 0.05$ versus control and CBI groups

could be observed between LC3-Beclin1, LC3-ZnT-2, Beclin1-ZnT2, Beclin1-ZnT3 and among ZnT1-ZnT3 in control group, while the linear correlations could be observed between LC3-Beclin1, Beclin1-ZnT2 and Beclin1-ZnT3 in RS group [5]. These data, combined with our present findings that anti-apoptotic protein bcl-2 down-regulated, strongly suggest that autophagic/apoptotic pathways may have been impacted at the protein level at the acute phase time point, which might be associated with the acute phase excitotoxicity and the long-term cognitive deficit.

Drug intervention remains the primary protocol for treatment of developmental seizure-induced pathological behavior, however, until now, to the best of our knowledge, no ideal drug intervention methods have been described. Recent findings from studies with adult animals have demonstrated that lysosomal enzyme cathepsin B is involved in apoptotic excitotoxicity. For example, Bhoopathi et al. showed that cathepsin B facilitates autophagy-mediated apoptosis in SPARC overexpressed primitive neuroectodermal tumor cells [25]. Houseweart et al. demonstrated that cathepsin B but not cathepsin L or S contributes to the pathogenesis of Unverricht-Lundborg progressive myoclonus epilepsy (EPM1) [26]. Canu et al. reported that apoptosis is accompanied by an early and marked proliferation of autophagosomal-lysosomal compartments involving cathepsin B following serum and potassium deprivation [27]. Other evidence supporting a role for cathepsin B in apoptosis comes from the finding that pharmacological inhibition of cathepsin B can block apoptosis. Cathepsin inhibitors can be protective in some models of neurodegeneration and could be therapeutic in ischemic injury, Alzheimer disease, and other protein deposition diseases in which compensatory responses by lysosomal enzymes may contribute to brain pathology [4, 28]. We have recently demonstrated that CBI could suppress activity of traumatic brain injury (TBI)-induced cathepsin B, which significantly suppressed plasmalemma
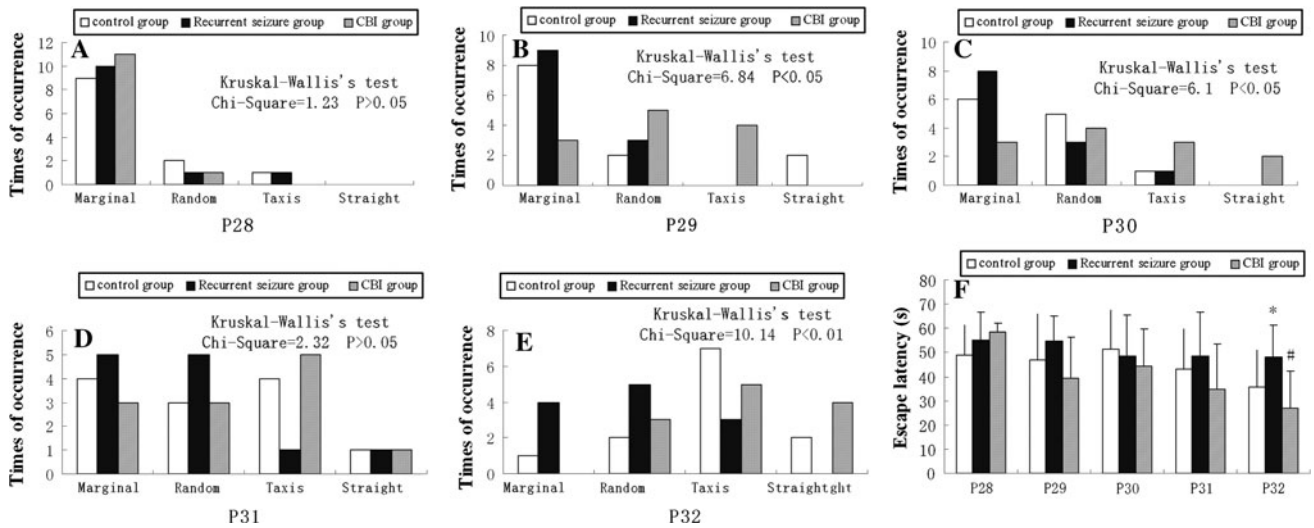
Fig. 4 Effects of CBI on recurrent neonatal seizure-induced cognitive deficits. Learning and memory function test was performed 14 days after injury by Morris water maze. There were more marginal strategy and less taxis strategy in RS group than that in CBI and control group in the second (Fig. 4b), third (Fig. 4c) and fifth day (Fig. 4e) ($P < 0.05$). The escape latencies from the water maze were significantly longer in rats of RS groups at d2 and d5 than that in CBI groups. $*P < 0.05$ versus control and CBI groups; $^{\#}P < 0.05$ versus RS group

Fig. 5 Real-time RT-PCR analysis of the expression of LC-3, Cathepsin-B and PRG-1 in hippocampus and cerebral cortex after behavioral analysis. $*P < 0.05$ versus control and CBI groups
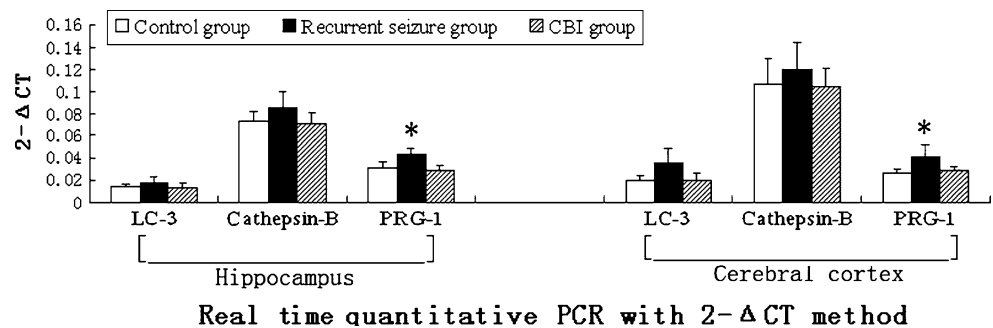
disruption, cell apoptosis, motor deficits, and cognitive dysfunctions (detected by Motor Test and Morris Water Maze) [8]. Our present experiment investigates the intervention effects of CBI on developmental seizure-induced cognitive and motor dysfunction. The results further suggest that CBI likely improves the learning and behavioral deficits caused by recurrent seizures in rats during brain development by modulating acute phase autophagic and apoptotic related gene and long-term PRG-1 expressions in hippocampus and cerebral cortex.

PRG-1 is a brain-specific membrane protein related to lipid phosphate phosphatases. It is specifically expressed in excitatory synapse terminating on glutamatergic neurons in hippocampus and entorhinal cortex. There, it is located in the membranes of outgrowing axons acts as an ectoenzyme and attenuates phospholipid-induced axon collapse in neurons and facilitates outgrowth in the hippocampus [29–31]. Deletion of *prg-1* in mice leads to epileptic seizures and augmentation of EPSCs, which suggests PRGs as important players in the modulatory control of

hippocampal excitability [31]. In a recently published paper from our laboratory, we reported for the first time that flurothyl inhalation-induced neonatal seizures caused significant elevation of PRG-1 expression in cerebral cortex 14 days after the last seizure [32]. This is just in accordance with our present results. Here, we showed upregulation of the PRG-1 in hippocampus and cerebral cortex only in adolescence after the last seizure (P35), this is just the time when the onset of regenerative mossy fiber spouting in forebrain could be observed following developmental seizures. Moreover, pre-treatment with CBI blocked seizure-induce expression upregulation of PRG-1 and subsequent cognitive deficit. So we can assume that PRG-1 might participate in the molecular mechanisms underlying neonatal recurrent seizure-induced long-term effects on behavioral dysfunction that merit further investigation.

In summary, the present study demonstrated, for the first time, that the autophagy/lososome and apoptosis signals are immediately activated in hippocampus and cerebral

cortex after recurrent neonatal seizures. These date and others support the hypothesis that lysosomal enzymes participate in neonatal seizure-induced brain damage and that modulation of cathepsin B may offer a new strategy for the development of therapeutic interventions for treatment of developmental seizure-induced brain damage.

References

1. Ben-Ari Y, Holmes GL (2006) Effects of seizures on developmental processes in the immature brain. Lancet Neurol 5:1055–1063

2. Holmes GL (2005) Effects of seizures on brain development: lessons from the laboratory. Pediatr Neurol 33:1–11

3. Holopainen IE (2008) Seizures in the developing brain: cellular and molecular mechanisms of neuronal damage, neurogenesis and cellular reorganization. Neurochem Int 52:935–947

4. Wang Y, Han R, Liang ZQ, Wu JC, Zhang XD, Gu ZL, Qin ZH (2008) An autophagic mechanism is involved in apoptotic death of rat striatal neurons induced by the non-N-methyl-D-aspartate receptor agonist kainic acid. Autophagy 4:214–226

5. Ni H, Feng X, Gong Y, Tao LY, Wu XR (2010) Acute phase expression pattern of ZnTs, LC3, and Beclin-1 in rat hippocampus and its regulation by 3-methyladenine following recurrent neonatal seizures. Biol Trace Elem Res doi: 10.1007/s12011-010-8836-5

6. Au AK, Bayir H, Kochanek PM, Clark RSB (2010) Evaluation of autophagy using mouse models of brain injury. Biochimica Biophysica Acta 1802:918–923

7. Zhang XD, Wang Y, Wu JC, Lin F, Han R, Han F et al (2008) Down-regulation of Bcl-2 enhances autophagy activation and cell death induced by mitochondrial dysfunction in rat striatum. J Neurosci Res 87:3600–3610

8. Luo CL, Chen XP, Yang R, Sun YX, Li QQ, Bao HJ, Cao QQ, Ni H, Qin ZH, Tao LY (2010) Cathepsin B contributes to traumatic brain injury-induced cell death through a mitochondria-mediated apoptotic pathway. J Neurosci Res 88:2847–2858

9. Kim R, Emi M, Tanabe K (2006) Role of mitochondria as the gardens of cell death. Cancer Chemother Pharmacol 57:545–553

10. de Roqalski Landrot I, Minokoshi M, Silveira DC, Cha BH, Holmes GL (2001) Recurrent neonatal seizures: relationship of pathology to the electroencephalogram and cognition. Brain Res Dev Brain Res 129:27–38

11. Ni H, Jiang YW, Tao LY, Jin MF, Wu XR (2009) ZnT-1, ZnT-3, CaMKII, PRG-1 expressions in hippocampus following neonatal seizure-induced cognitive deficit in rats. Toxico Lett 184:145–150

12. Ni H, Jiang YW, Tao LY, Cen JN, Wu XR (2009) Effects of penicillin-induced developmental epilepticus on hippocampal regenerative sprouting, related gene expression and cognitive deficits in rats. Toxico Lett 188:161–166

13. Ni H, Li C, Tao LY, Cen JN (2009) Physical exercise improves learning by modulating hippocampal mossy fiber sprouting and related gene expression in a developmental rat model of penicillin- induced recurrent epilepticus. Toxicol Lett 191:26–32

14. Ni H, Jiang YW, Bo T, Wang JM, Pan H, Wu XR (2004) Long-term effects of neonatal seizures on subsequent NMDA-1 and GABA-A-α1 receptor expression in hippocampus of the Wistar rat. Neurosci Lett 368:254–257

15. Ni H, Jiang YW, Bo T, Wang JM, Wu XR (2005) C-Fos, N-methyl-D-aspartate receptor 2C, GABA-A-1 immono-reactivity, seizure latency and neuronal injury following single or recurrent neonatal seizures in hippocampus of Wistar rat. Neurosci Lett 380:149–154

16. Holmes GL, Gairsa JL, Chevassus-Au-Louis N, Ben-Ari Y (1998) Consequences of neonatal seizures in the rat: morphological and behavioral effects. Ann Neurol 44:845–857

17. Bengzon J, Mohapel P, Ekdahl CT, Lindvall O (2002) Neuronal apoptosis after brief and prolonged seizures. Prog Brain Res 135:111–119

18. Cao L, Xu J, Lin Y, Zhao X, Liu X, Chi Z (2009) Autophagy is upregulated in rats with status epilepticus and partly inhibited by Vitamin E. Biochem Biophys Res Commun 379:949–953

19. Kabeya Y, Mizushima N, Ueno T, Yamamoto A, Kirsako T, Noda T et al (2000) LC3, a mammalian homologue of yeast Apg8p, is located in autophagosome membranes after processing. EMBO J 19:5720–5728

20. Kihara A, Kabeya Y, Ohsumi Y, Yoshimori T (2001) Beclin-phosphatidylinositol 3- kinase complex functions at the trans-Golgi network. EMBO Rep 2:330–335

21. Diskin T, Tal-Or P, Erlich S, Mizrachy L, Alexandrovich A, Shohami E et al (2005) Closed head injury induces upregulation of Beclin 1 at the cortical site of injury. J Neurotrauma 22:750–762

22. Yan L, Sadoshima J, Vatner DE, Vatner SF (2006) Autophagy: a novel protective mechanism in chronic ischemia. Cell Cycle 5:1175–1177

23. Rami A, Langhagen A, Steiger S (2008) Focal cerebral ischemia induces upregulation of Beclin 1 and autophagy-like cell death. Neurobiol Dis 29:132–141

24. Carloni S, Buonocore G, Balduini W (2008) Protective role of autophagy in neonatal hypoxia-ischemia induced brain injury. Neurobio Dis 32:329–339

25. Bhoopathi P, Chetty C, Gujrati M, Dinh DH, Rao JS, Lakka S (2010) Cathepsin B facilitates autophagy-mediated apoptosis in SPARC overexpressed primitive neuroectodermal tumor cells. Cell Death Differ 17:1529–1539

26. Houseweart MK, Pennacchio LA, Vilaythong A, Peters C, Noebels JL, Myers RM (2003) Cathepsin B but not cathepsins L or S contributes to the pathogenesis of Unverricht-Lundborg progressive myoclonus epilepsy (EPM1). J Neurobiol 56:315–327

27. Canu N, Tufi R, Serafino AL, Amadoro G, Ciotti MT, Calissano P (2005) Role of the autophagic-lysosomal system on low potassium-induced apoptosis in cultured cerebellar granule cells. J Neurochem 92:1228–1242

28. Bendiske J, Bahr BA (2003) Lysosomal activation is a compensatory response against protein accumulation and associated synaptopathogenesis-An approach for slowing Alzheimer disease. J Neuropathol Exp Neurol 62:451–463

29. Brauer AU, Savaskan NE, Kuhn H, Prehn S, Ninnemann O, Nitsch R (2003) A new phospholipid phosphatase, PRG-1, is involved in axon growth and regenerative sprouting. Nat Neurosci 6:572–578

30. Brauer AU, Nitsch R (2008) Plasticity-related genes (PRGs/LRPs): a brain-specific class of lysophospholipid-modifying proteins. Biochimica et Biophysica Acta-Molecul Cell Biol Lipids 1781:595–600

31. Thorsten T, Prateep B, Johannes V (2009) Synaptic PRG-1 modulates excitatory transmission via lipid phosphate-mediated signaling. Cell 138:1222–1235

32. Ni H, Jiang YW, Xiao ZJ, Tao LY, Jin MF, Wu XR (2010) Dynamic pattern of gene expression of ZnT-1, ZnT-3 and PRG-1 in rat brain following flurothyl-induced recurrent neonatal seizures. Toxicol Lett 194:86–93